The Astrophysical Journal Letters, 733:L3 (5pp), 2011 May 20 doi:10.1088/2041-8205/733/1/L3

COLLISIONAL EXCAVATION OF ASTEROID (596) SCHEILA

D. Bodewits[1], M. S. Kelley[1], J.-Y. Li[1], W. B. Landsman[2], S. Besse[1], and M. F. A'Hearn[1]
[1] Department of Astronomy, University of Maryland, College Park, MD 20742, USA; dennis@astro.umd.edu, msk@astro.umd.edu, jyli@astro.umd.edu, sbesse@astro.umd.edu, ma@astro.umd.edu
[2] NASA GSFC, Adnet Systems, Mailstop 667, Greenbelt, MD 20771, USA; Wayne.B.Landsman@nasa.gov
Received 2011 January 26; accepted 2011 March 24; published 2011 April 28

ABSTRACT

We observed asteroid (596) Scheila and its ejecta cloud using the *Swift* UV–optical telescope. We obtained photometry of the nucleus and the ejecta, and for the first time measured the asteroid's reflection spectrum between 290 and 500 nm. Our measurements indicate significant reddening at UV wavelengths (13% per 10^3 Å) and a possible broad, unidentified absorption feature around 380 nm. Our measurements indicate that the outburst has not permanently increased the asteroid's brightness. We did not detect any of the gases that are typically associated with either hypervolatile activity thought responsible for cometary outbursts (CO^+, $CO_2{}^+$), or for any volatiles excavated with the dust (OH, NH, CN, C_2, C_3). We estimate that 6×10^8 kg of dust was released with a high ejection velocity of 57 m s^{-1} (assuming 1 μm sized particles). While the asteroid is red in color and the ejecta have the same color as the Sun, we suggest that the dust does not contain any ice. Based on our observations, we conclude that (596) Scheila was most likely impacted by another main belt asteroid less than 100 m in diameter.

Key words: minor planets, asteroids: individual ((596) Scheila) – ultraviolet: planetary systems

Online-only material: color figures

1. INTRODUCTION

Early 2010 December, an unexpected dust cloud was discovered around the asteroid (596) Scheila (Larson et al. 2010). We report on observations using the UV–Optical Telescope (UVOT) on board *Swift*.

Asteroids have long been believed to be currently geologically inactive. Instead, their shapes, sizes, and surface geology are dominated by impacts. However, several asteroids have been observed to develop a coma and or dust tail (Hsieh & Jewitt 2006). Some asteroids are repeatedly active over periods as long as months, most famously 133P/Elst-Pizzaro (Hsieh et al. 2004). Others are only active in short-lived bursts. Two main ejecta processes have been suggested: cometary-like outgassing of volatiles driven by an exoergic interior process (Jewitt 2009) and inter-asteroidal collisions (Jewitt et al. 2010; Snodgrass et al. 2010). Alternatively, collisions may expose icy content buried beneath the surface (Hsieh et al. 2004).

(596) Scheila is a T-type main belt asteroid with a diameter of 113 km.[3] On 2010 December 11.44 UT the asteroid had increased by $m_v = 0.8$ and archival Catalina Sky Survey observations showed that the activity was triggered between 2010 November 11 and December 3 (Larson et al. 2010). The asteroid orbits the Sun in 5.0 yr with an eccentricity of 0.16 and a semimajor axis of 2.93 AU. Its outburst occurred at $r_h = 3.1$ AU, close to its aphelion at 3.4 AU. Scheila offered a unique target as we observed it only weeks after its outburst; the outburst of P/2010 A2 (Linear) was discovered in 2010 January (Birtwhistle et al. 2010), almost a year after it was triggered (Jewitt et al. 2010; Moreno et al. 2010; Snodgrass et al. 2010).

2. OBSERVATIONS

Swift is a multi-wavelength observatory equipped for rapid follow-up of gamma-ray bursts (Gehrels et al. 2004). Our observations use the UVOT that provides a 17 × 17 arcminute field of view with a plate scale of 1 arcsec pixel^{-1} and a point-spread function of 2.″5 FWHM (Mason et al. 2004). Seven broadband filters allow color discrimination, and two grisms provide low-resolution ($\lambda/\delta\lambda = 100$) spectroscopy between 170 and 650 nm.

Swift observed (596) Scheila on 2010 December 14 and 15 UT (Table 1). On both days we used the *V* (λ_c 546.8 nm, FWHM 75.0 nm) and *UVW*1 (λ_c 260.0 nm, FWHM 70.0 nm) filters. On December 15 we used the UV grism to search for gaseous emission lines. The grism was operated in "clocked mode" to suppress background stars and the dispersion axis was oriented at a position angle of ∼260°. The asteroid was not tracked, and the proper motion is 6.″2 over our ∼1300 s exposures.

The results are subject to several possible systematic uncertainties. The absolute calibration of UVOT[4] is accurate to within 0.01 mag (*V*) and 0.03 mag (*UVW*1). The brightness of the nucleus results in significant coincidence loss that we estimate to be 0.3 ± 0.05 mag at *V* and 0.02 ± 0.005 mag at *UVW*1. Shot noise and background subtraction uncertainty, as well as the aperture and coincidence loss correction errors, are all included in the listed uncertainties.

3. RESULTS

3.1. Imaging

The images obtained with the *V* and *UVW*1 broadband filters were registered, binned, and logarithmically stretched to allow inspection of the morphology of the ejecta (Figure 1). Both panels span about 215″ × 204″, corresponding to 390,000 × 370,000 km. We used archival DSS[5] images to identify and remove background sources. The projected directions to the Sun and the orbital motion almost coincide and are indicated by arrows.

[3] http://ssd.jpl.nasa.gov/sbdb.cgi

[4] http://swift.gsfc.nasa.gov/docs/swift/analysis/uvot_digest/zeropts.html

[5] Digitized Sky Survey; see http://archive.stsci.edu/cgi-bin/dss_form

Table 1
Observing Log and Photometry Results

Start Observing Time (UT)	Filter	Exp. Time (s)	m Nucleus[a]	m Ejecta[a,b] ($160'' \times 100''$)	m Ejecta[a,b] ($80'' \times 80''$)
2010 Dec 14 T06:47	*V*	1285	14.1 ± 0.05	14.4 ± 0.06	14.8 ± 0.06
2010 Dec 14 T07:09	*UVW*1	701	16.4 ± 0.07	-	16.7 ± 0.08
2010 Dec 15 T06:56	*UV* grism	1072	14.3 ± 0.1	-	-
2010 Dec 15 T08:29	*V*	1300	14.0 ± 0.05	14.3 ± 0.06	14.9 ± 0.06
2010 Dec 15 T08:50	*UVW*1	1087	16.3 ± 0.04	-	16.8 ± 0.08

Notes.
[a] Errors include both stochastic and absolute uncertainties.
[b] The *UVW*1 ejecta are faint and best measured in the smaller $80'' \times 80''$ aperture to minimize background stars and the systematic uncertainty.

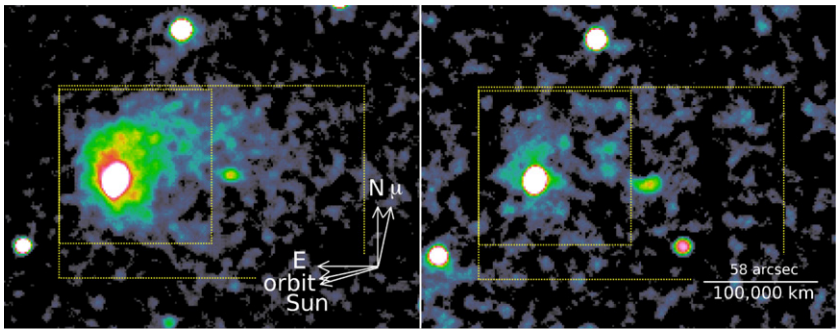

Figure 1. UVOT images obtained with the *V* (left) and *UVW*1 (right) filters on 2010 December 15 UT. The physical scale and orientation are the same in both frames. Both images are scaled logarithmically, but stretched and smoothed separately to enhance the ejecta. The untracked asteroid appears slightly elongated in the northward direction (μ). Two plumes can be seen, and their morphology is consistent with ejecta moving away from the asteroid and then being pushed in the anti-solar direction by solar radiation pressure. The yellow boxes indicate the area from which we obtained the color (small) and total (large) photometry.
(A color version of this figure is available in the online journal.)

We have clearly resolved detections of the ejecta in both filters. In the *V* band, the morphology seems to consist of a broad "northern" fan from position angle (P.A.) = 330° to 60°, and a curved "southern" feature at P.A. = 180°.

Aperture photometry on the images yields an average $m_v = 14.1 \pm 0.07$ and $m_{uv} = 16.4 \pm 0.09$ for the asteroid in a 10 pixel radius aperture. We made no attempt to remove the dust emission within our asteroid aperture. Subtracting the nucleus' brightness, the total dust brightness in a $160'' \times 100''$ aperture is $m_v = 14.4 \pm 0.08$. The northern plume is brighter than the southern plume (65% versus 35% of the total ejecta flux). The ejecta are faint in *UVW*1 (Figure 1) and best measured in a smaller $80'' \times 80''$ aperture to minimize uncertainties from the background subtraction. We find an average $m_v = 14.8 \pm 0.08$ and $m_{uv} = 16.8 \pm 0.11$ for the ejecta in the smaller aperture (Table 1 and Figure 1). Our measurements are close to the asteroid's predicted brightness ($m_v = 14.21$,[6] with an estimated maximum amplitude of 0.09).[7] Within the uncertainties, the ejecta (*UVW*1–*V* = 1.91 ± 0.1) have solar colors (*UVW*1–*V* = 1.94), while the asteroid (*UVW*1–*V* = 2.36 ± 0.11) is redder than the Sun.

3.2. Spectroscopy

Figure 2 shows the asteroid's spectrum extracted from a rectangular region 13 pixels wide along with a solar spectrum obtained on 2010 December 15 (SORCE; McClintock et al. 2005).[8] The spectrum below 280 nm was contaminated by a background star. The data were binned by a factor of eight to improve the signal to noise, and to suppress the Mod8 pattern in the grism image. For comparison, the grism spectrum of comet C/2007 N3 (Lulin) is shown in Figure 2 (Bodewits et al. 2011). While Lulin's spectrum is dominated by the emission features of several gaseous species (e.g., OH, CN, C_2, C_3, NH, CO_2^+), there is no evidence of any gaseous emission feature in the asteroid's spectrum. Assuming an OH fluorescence feature similar to that

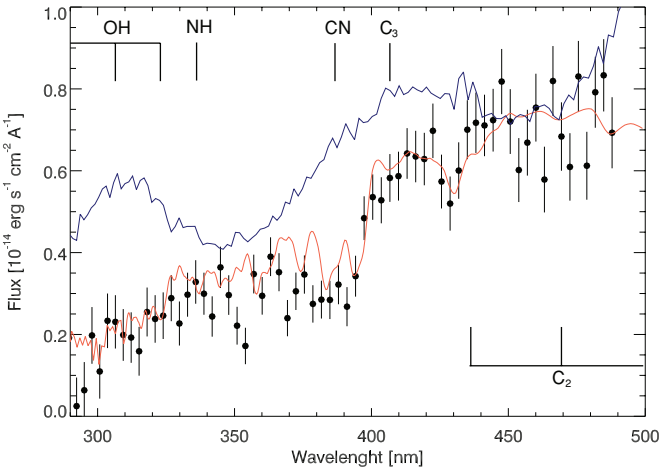

Figure 2. Spectra of Scheila (black), comet C/2007 N3 (Lulin) (blue; Bodewits et al. 2011) normalized at 450 nm and the Sun (red; McClintock et al. 2005), scaled to $m_v = 14.3$. Scheila's spectrum is reddened compared to the Sun. There is no evidence of volatile emission lines that dominate Lulin's spectrum (labeled). Error bars indicate 1σ stochastical errors; the systematic uncertainty is approximately 25%.
(A color version of this figure is available in the online journal.)

[6] http://ssd.jpl.nasa.gov/?horizons
[7] http://sbn.psi.edu/ferret/
[8] http://lasp.colorado.edu/lisird/sorce/sorce_ssi/index.html

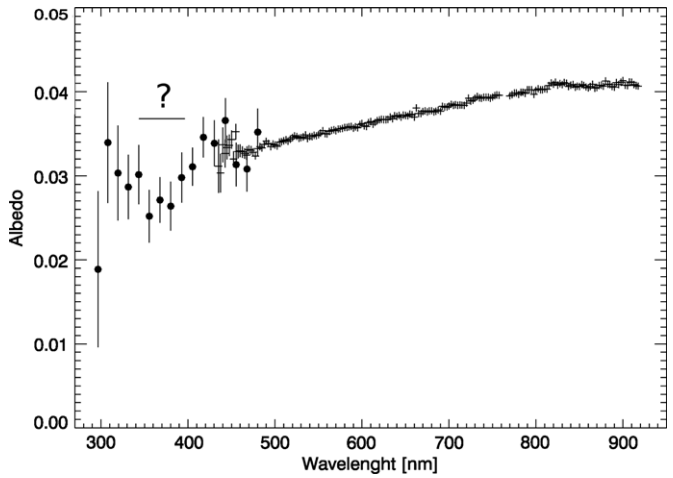

Figure 3. Albedo of Scheila. (•) *Swift* measurements; (+) reflectance measurements by Bus & Binzel (2002), scaled to match our albedo measurement. Error bars indicate 1σ stochastical errors. Our data are in excellent agreement with other albedo measurements. We tentatively identify a broad absorption feature between 320 and 420 nm, indicated by the question mark.

in Lulin's spectrum (50 nm wide due to the gas distribution), a 1σ flux upper limit of 1×10^{-13} erg s^{-1} cm^{-2} A^{-1}, and a total OH emission fluorescence of 2.2×10^{-16} erg s^{-1} cm^{-2} molecule^{-1} (Schleicher & A'Hearn 1988) yields an upper limit 3×10^{30} OH molecules around the nucleus. Considering the long lifetime of OH at 3.1 AU from the Sun ($\sim 10^6$ s; Huebner et al. 1992), the water production rate would be $<10^{25}$ molecules s^{-1}, 1000 times lower than typically observed in Jupiter family comets at 1 AU. Although we cannot constrain the gaseous output at the onset of the anomaly, we conclude that the asteroid did not produce significant OH or water gas during the observations.

Scaling the solar spectrum yields a best fit of $m_v = 14.3 \pm 0.1$, in agreement with our broadband observations. We derived the asteroid's albedo using Equation (2), assuming $\Phi(\alpha) = 0.45$, a diameter of 113 km (Dunham & Herald 2005),[7] and the solar irradiance from SORCE (Figure 3). We combined this with a scaled reflectance spectrum (Bus & Binzel 2002).[7] Our data are in excellent agreement with albedo measurements from other observations (Dunham & Herald 2005[6]; Ryan & Woodward 2010). Scheila's spectrum is significantly reddened compared to the Sun.

There appears to be a broad absorption feature between 320 and 420 nm, centered at about 380 nm, superimposed on the red slope. It is difficult to interpret the UV spectrum of Scheila due to both the limited number of asteroids observed at this wavelength (Butterworth & Meadows 1985; Roettger & Buratti 1994), and due to the lack of laboratory reflectance spectra of possible compositional minerals. UV absorptions at slightly shorter wavelengths are present with various intensities for possibly hydrated asteroids such as (1) Ceres, (2) Pallas, and (102) Hygiea (Butterworth & Meadows 1985; Roettger & Buratti 1994; Li et al. 2006, 2009; Rivkin et al. 2006; Milliken & Rivkin 2009). UV spectra of S-types show a strong red slope and sharp drop at 300–400 nm, and very weak UV absorptions. As a primitive-type asteroid in the outer main asteroid belt with $\sim$4% albedo, Scheila probably has a surface composition that is closer to carbonaceous meteorites. In order to better understand the UV spectra of asteroids, observations of various spectral types and laboratory measurements of carbonaceous meteorites are needed.

4. DISCUSSION

4.1. Ejecta Dynamics

The sunward extend of the cloud is $\sim 15''$, corresponding to 2.6×10^4 km at the asteroid. This is the distance X_R where solar radiation turns dust particles, and it can be used to estimate the grain ejection velocity (Hsieh et al. 2004; Jewitt & Meech 1987):

$$X_R \sim \frac{v_d^2 r_h^2}{2\beta_d g_{\rm sun}}, \quad (1)$$

where v_d is the relative ejection velocity, r_h is the heliocentric distance in AU, β is the dimensionless ratio between radiation pressure acceleration and the local gravity, and $g_{\rm sun} = 0.006$ m s^{-2} is the gravitational acceleration to the Sun at 1 AU. Using this we find $v_d = 57\sqrt{\beta}$ m s^{-1}.

This velocity is an order of magnitude larger than those reported for 133P ($1.5\sqrt{\beta}$ m s^{-1}; Hsieh et al. 2004) and P/2010 A2 ($1.1\sqrt{\beta}$ m s^{-1}; Moreno et al. 2010). This difference is partially explained by the different escape velocities. Assuming a density of 2500 kg m^{-3}, and the estimated diameters (113 km versus 0.12 km), the escape velocities are 75 m s^{-1} for 596 and 0.06 m s^{-1} for P/2010 A2. Additionally, the collision disrupting A2 may have produced a lot of high-velocity dust, but this had left the vicinity of A2 over the year between the impact and its discovery.

We simulated the ejection of dust from 596 to better understand the dynamics of the observed ejecta. The simulation accounts for the gravitational acceleration of the Sun and planets and solar radiation pressure (Kelley 2006; Kelley et al. 2009). The model was designed to simulate observations of comet comae, and does not account for the mass of the parent body. Since 596 is a large asteroid, our simulation is only a rough approximation to the true dust ejection dynamics. We ejected 10^6 grains isotropically from the surface in a single event, with a distribution of sizes (0.1–10^4 μm) and velocities (0–100 m s^{-1}) on 2010 December 3, and integrated their positions forward in time to 2010 December 15. The full extent of the dust in our UVOT images can be encompassed in a circle centered on the asteroid with a radius of $76''$ (140,000 km). Our simulations show that 12 days after the outburst, only grains >1 μm in radius remain within this aperture. Therefore, we adopt 1 μm as a lower limit to the ejected grain size. A stricter limit to the grain radii can be estimated if the outburst date can be better constrained, and if the dynamics of the ejecta could be reproduced, neither of which have we attempted. Independent of these refinements, all grains smaller than ~ 1 μm would be found outside the observed extent of the dust in our *V*-band image. Therefore, we conclude that sub-micron-sized grains are few or absent in the ejecta.

We continued our simulation forward in time with 10-day steps to estimate the lifetime of the ejecta within our $76''$ radius aperture. We have weighted the dust grain cross sections by v^{-1} to approximate crater formation dynamics (more mass is ejected at lower velocities), and converted cross section to *V*-band magnitudes using Equation (2) (Figure 4). The evolution of the dust results in a rapid decline of m_v of approximately 3 mag over the first month. If the ejecta are devoid of large grains (i.e., the grain-size upper limit is 10 μm, rather than our initial assumption of 10^4 μm), then the dust will be even fainter, falling 5 mag by mid-January. According to our simulations, unless the grain radii extend at least into the millimeter size range, we expect that the surface brightness of the ejecta cloud around Scheila will be too faint to observe in early 2011.

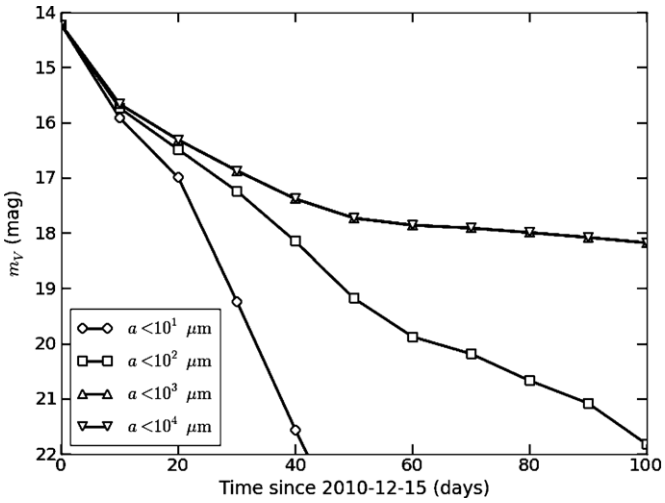

Figure 4. Simulated apparent *V*-band magnitude of dust within 76″. Light curves are given for grain radius upper limits of 10–10^4 μm. The larger radiation pressure efficiency of smaller grains removes them from the field of view quickly, reducing the reflection cross section of the dust. We expect that the surface brightness of the ejecta cloud will soon be too faint to observe.

4.2. Dust Mass

The total reflection cross section C_d is related to the difference between the *V*-band magnitudes of dust and the apparent solar magnitude ($m_{\rm sun} = -26.74$) by the following relation:

$$C_d = 2.25 \times 10^{22} \pi \frac{r_h^2 \Delta^2 10^{-0.4(m_d - m_{\rm sun})}}{p_V \Phi(\alpha)}, \quad (2)$$

where the heliocentric distance $r_h = 3.1$ AU, the geocentric distance $\Delta = 2.5$ AU, p_V is the geometric albedo, and $\Phi(\alpha)$ is the phase darkening. Assuming a phase correction of 0.75 for a solar phase angle of 16° (Schleicher et al. 1998), and a dust albedo of 0.1 (Jewitt 2009), we find $C_d \sim 2 \times 10^9$ m^2 for the ejecta. Further assuming a power-law distribution of spherical particles with radii between 10^{-6} and 10^{-2} m (Section 4.1), with a slope of −3.5, and a density of 2500 kg m^{-3}, we can use the relation between mass and scattering cross section derived by Jewitt (2009). We then find that there was approximately 6×10^8 kg of dust around the asteroid.

To put this in perspective, this is a much larger mass than found around active centaurs (10^4–10^6 kg; Jewitt 2009), comparable to the mass released by the destruction of P/2010 A2 (LINEAR) (5–60 $\times$ 10^7 kg; Moreno et al. 2010; Snodgrass et al. 2010; Jewitt et al. 2010), and comparable to the total amount of dust and gas excavated by the Deep Impact probe colliding with 9P/Tempel 1 (10^6–10^9 kg; Küppers et al. 2005; A'Hearn 2008).

4.3. Asteroid Impact Scenario

We did not detect any evidence of volatiles that are typically associated with the hypervolatile activity (CO^+, CO_2^+), or of any volatiles that were possibly released from the ejected dust (OH, NH, CN, C_2, C_3). The reddening of the asteroid (13% per 10^3 Å) and the neutral color of the ejecta are comparable to those of comet surfaces and comae, which are generally considered to be ice free. Comets 9P/Tempel-1, 21P/Giacobini–Zinner, and 67P/Churyumov–Gerasimenko have nucleus spectral reflectivity gradients of 12.5% ± 1%, 12.8% ± 2.7%, and 11% ± 2%, and comae gradients of about 8%, 8% ± 3%, and −1% to 1%, respectively (Li et al. 2007; Luu et al. 1993; Tubiana et al. 2008; Schleicher 2007; Kolokolova et al. 1997; Weiler et al. 2004; Lara et al. 2005). We therefore conclude that there were no detectable amounts of gas or ice around the asteroid during our observations. However, most fragment species observed in optical/UV wavelengths have lifetimes corresponding to about 11.1 days at the heliocentric distance of the asteroid (Huebner et al. 1992). Icy grains have even shorter lifetimes (Bockelée-Morvan et al. 2001). While we cannot rule out that gas or ice was released at the onset of the outburst (before December 3), our results do imply that the excavation event did not trigger any continuous activity.

The plumes are consistent with ejecta moving away from the asteroid and then being pushed along the anti-solar direction by solar radiation pressure. The observed morphology could be well explained by an oblique impact where one plume would be associated with downrange ejecta and the other with material ejected vertically due to the mechanical excavation by shockwaves generated by the impact (see, e.g., Schultz et al. 2007).

We estimated above that about 6×10^8 kg of dust was released. Assuming a density of 2500 kg m^{-3}, this corresponds to a sphere with a diameter of 80 m. If we assume that most of the momentum input from the impact is carried out by the ejecta, and an impact velocity of 5 km s^{-1}, we find an impact diameter of 20 m, consistent with our first estimate. If the observed dust was indeed ejected by an impact, then the ejecta probably constitute only 10%–20% of the total excavated mass. The mass of the material excavated by hypervelocity impacts usually exceeds the mass of the projectile, depending on many parameters such as the impact velocity and geometry, porosity, and the strength of the target (Holsapple et al. 2002; Schultz et al. 2005). We conclude that the projectile was therefore probably <100 m in diameter.

How likely is this collision scenario? Asteroid collisions have been extensively studied for evolution studies (Bottke et al. 1994; Davis et al. 2002). In the main belt, the most likely collision partners are other main belt asteroids. Bottke et al. (1994) give an intrinsic collision probability of 3×10^{-18} yr^{-1} km^{-2} at a relative velocity of 5.3 km s^{-1}. Multiplying this with the square of the radius of Scheila and *N*, the number of projectiles sized 10–100 m, yields the impact frequency. A compilation of different distribution models suggests that the number of projectiles is in the range 10^{10}–10^{11} (Davis et al. 2002). Based on this estimate, an object the size of (596) Scheila would be impacted by a small asteroid once every 1000 years. There are ∼200 asteroids the size of (596) Scheila (Tedesco et al. 2004), thus an event like this would occur once every five years, and collisions with asteroids smaller than 10 m should occur even more often. Based on statistics, a collisional impact is thus very likely.

More tentatively, it is possible to estimate what effect the impact had on the surface of Scheila. Craters on (243) Ida, (951) Gaspra, (25143) Itokawa, (2867) Steins, and (443) Eros have different depth-to-diameter ratios that are linked to the history of the asteroid itself (Sullivan et al. 1996; Carr et al. 1994; Hirata et al. 2009; Besse et al. 2011; Robinson et al. 2002). Assuming spherical craters, the diameter *D* is related to the volume $V \sim 0.06\ D^3$ (Scheeres et al. 2002; depth-to-diameter ratio of 0.15). Based on the equivalent volume of the ejecta (3×10^5 m^3), and considering that the ejected mass may only constitute 10%–20% of the total excavated mass, the impact may have resulted in a crater with a diameter of 300 m. Fresh craters often have a higher depth-to-diameter ratio than aged craters; consequently the impact may well have created a

crater with a diameter much larger than 300 m. An impact of that size is not unexpected on the surface of asteroids. During its recent flyby of the asteroid (21) Lutetia, which has a size comparable to (596) Scheila, the *Rosetta* spacecraft discovered numerous craters with diameters larger than 500 m, likely the scars of impacts similar to that occurred on (596) Scheila.

5. CONCLUSIONS

We obtained optical and UV images and spectroscopy of asteroid (596) Scheila using the *Swift* UVOT within at most six weeks after it first started to show a dramatic increase in brightness. We obtained the first measurement of its reflectance spectra below 450 nm, a wavelength regime in which asteroids are not very well explored. Whatever caused the ejection of dust from Scheila has not permanently increased the asteroid's brightness. We did not detect any of the gases that are typically associated with either hypervolatile activity thought responsible for cometary outbursts (CO^+, $CO_2{}^+$), or for any volatiles excavated with the dust (OH, NH, CN, C_2, C_3). We estimate that 6×10^8 kg of dust was released with an ejection velocity of 57 m s^{-1} (assuming 1 μm sized particles). The ejecta have the same color as the Sun, while the asteroid appears reddened. The two colors are consistent with observations of comet comae and nuclei, both generally considered to be ice-free. Based on our observations, we conclude that Scheila was most likely impacted by another main belt asteroid with a diameter of at most 100 m.

We thank the *Swift* team for use of Director's Discretionary Time and for the careful and successful planning of these observations. We thank Pete Schultz for valuable discussions on this study.

Note added in proof. During the proofing stage of this paper, we became aware of a manuscript describing recent *Hubble Space Telescope* observations of Scheila's outburst event by Jewitt et al. (2011). That paper independently reaches conclusions similar to those presented here and appears in the same issue of the journal.

REFERENCES

A'Hearn, M. F. 2008, Space Sci. Rev., 138, 237
Besse, S., et al. 2011, Icarus, submitted
Birtwhistle, P., Ryan, W. H., Sato, H., Beshore, E. C., & Kadota, K. 2010, IAU Circ., 9105, 1
Bockelée-Morvan, D., et al. 2001, Science, 292, 1339
Bodewits, D., Villanueva, G. L., Mumma, M. J., Landsman, W. B., Carter, J. A., & Read, A. M. 2011, AJ, 141, 12
Bottke, W. F., Nolan, M. C., Greenberg, R., & Kolvoord, R. A. 1994, Icarus, 107, 255
Bus, S. J., & Binzel, R. P. 2002, Icarus, 158, 1
Butterworth, P. S., & Meadows, A. J. 1985, Icarus, 62, 305
Carr, M. H., Kirk, R. L., McEwen, A., Veverka, J., Thomas, P., Head, J. W., & Murchie, S. 1994, Icarus, 107, 61
Davis, D. R., Durda, D. D., Marzari, F., Campo, B., & Gil-Hutton, R. 2002, in Asteroids III, ed. W. F. Bottke, Jr. et al. (Tucson, AZ: Univ. Arizona Press), 545
Dunham, D. W., & Herald, D. 2005, Asteroid Occultation List, NASA Planetary Data System, EAR-A-3-RDR-OCCULTATIONS-V3.0:OCCLIST_TAB
Gehrels, N., et al. 2004, ApJ, 611, 1005
Hirata, N., et al. 2009, Icarus, 200, 486
Holsapple, K., Giblin, I., Housen, K., Nakamura, A., & Ryan, E. 2002, in Asteroids III, ed. W. F. Bottke, Jr. et al. (Tucson, AZ: Univ. Arizona Press), 443
Hsieh, H. H., & Jewitt, D. C. 2006, Science, 312, 561
Hsieh, H. H., Jewitt, D. C., & Fernandez, Y. R. 2004, AJ, 127, 2997
Huebner, W. F., Keady, J. J., & Lyon, S. P. 1992, Ap&SS, 195, 1
Jewitt, D., Weaver, H. A., Agarwal, J., Mutchler, M., & Drahus, M. 2010, Nature, 467, 817
Jewitt, D., Weaver, H., Mutchler, M., Larson, S., & Agarwal, J. 2011, ApJ, 733, L4
Jewitt, D. C. 2009, AJ, 137, 4296
Jewitt, D. C., & Meech, K. J. 1987, ApJ, 317, 992
Kelley, M. S. 2006, PhD thesis, Univ. Minnesota, Minneapolis, MN
Kelley, M. S., Wooden, D. H., Tubiana, C., Boehnhardt, H., Woodward, C. E., & Harker, D. E. 2009, AJ, 137, 4633
Kolokolova, L., Jockers, K., Chernova, G., & Kiselev, N. 1997, Icarus, 126, 351
Küppers, M., et al. 2005, Nature, 437, 987
Lara, L. M., de Leon, J., Licandro, J., & Gutierrez, P. J. 2005, Earth Moon Planets, 97, 165
Larson, S., Kowalski, R., Sato, H., Yoshimoto, K., & Nakano, S. 2010, CBET, 2583, 1
Li, J.-Y., McFadden, L. A., A'Hearn, M. F., Feaga, L. M., Russell, C. T., Coradini, A., De Sanctis, C., & Ammannito, E. 2009, in 40th Lunar and Planetary Science Conf. (Houston, TX: LPI), abstract 2101
Li, J.-Y., McFadden, L. A., Parker, J. Wm., Young, E. F., Stern, S. A., Thomas, P. C., Russell, C. T., & Sykes, M. V. 2006, Icarus, 182, 143
Li, J.-Y., et al. 2007, Icarus, 187, 41
Luu, J. X. 1993, Icarus, 104, 138
Mason, K. O., Breeveld, A., Hunsberger, S. D., James, C., Kennedy, T. E., Roming, P. W. A., & Stock, J. 2004, in UV, X-Ray, and Gamma-Ray Space Instrumentation for Astronomy XIII, Vol. 5165, ed. K. A. Flanagan & O. H. W. Siegmund (Bellingham, WA: SPIE), 277
McClintock, W. E., Rottmann, G. J., & Woods, T. N. 2005, Sol. Phys., 230, 225
Milliken, R. E., & Rivkin, A. S. 2009, Nat. Geosci., 2, 258
Moreno, F., et al. 2010, ApJ, 718, L132
Rivkin, A. S., Volquardsen, E. L., & Clark, B. E. 2006, Icarus, 185, 563
Robinson, M. S., Thomas, P. C., Veverka, J., Murchie, S. L., & Wilcox, B. B. 2002, Meteorit. Planet. Sci., 37, 1651
Roettger, E. E., & Buratti, B. J. 1994, Icarus, 112, 496
Ryan, E. L., & Woodward, C. E. 2010, AJ, 140, 933
Scheeres, D. J., Durda, D. D., & Geissler, P. E. 2002, in Asteroids III, ed. W. F. Bottke, Jr. et al. (Tucson, AZ: Univ. Arizona Press), 527
Schleicher, D. G. 2007, Icarus, 190, 406
Schleicher, D. G., & A'Hearn, M. F. 1988, ApJ, 331, 1058
Schleicher, D. G., Millis, R. L., & Birch, P. V. 1998, Icarus, 132, 397
Schultz, P. H., Clara, A., Eberhardy, C. M., A'Hearn, M. F., Sunshine, J. M., & Lisse, C. M. 2007, Icarus, 190, 295
Schultz, P. H., Ernst, C. M., & Anderson, J. L. B. 2005, Space Sci. Rev., 117, 207
Snodgrass, C., et al. 2010, Nature, 467, 814
Sullivan, R., et al. 1996, Icarus, 120, 119
Tedesco, E. F., Noah, P. V., Noah, M., & Price, S. D. 2004, IRAS Minor Planet Survey, V6.0, NASA Planetary Data System, IRAS-A-FPA-3-RDR-IMPS-V6.0
Tubiana, C., Barrera, L., Drahus, M., & Boehnhardt, H. 2008, A&A, 490, 377
Weiler, M., Rauer, H., & Helbert, J. 2004, A&A, 414, 749